Basic Res Cardiol (2011) 106:1173–1191
DOI 10.1007/s00395-011-0222-8

ORIGINAL CONTRIBUTION

Chronic akt activation accentuates aging-induced cardiac hypertrophy and myocardial contractile dysfunction: role of autophagy

Yinan Hua · Yingmei Zhang · Asli F. Ceylan-Isik · Loren E. Wold · Jennifer M. Nunn · Jun Ren

Received: 18 May 2011 / Revised: 9 August 2011 / Accepted: 1 September 2011 / Published online: 9 September 2011

Abstract Aging is often accompanied with geometric and functional changes in the heart, although the underlying mechanisms remain unclear. Recent evidence has described a potential role of Akt and autophagy in aging-associated organ deterioration. This study was to examine the impact of cardiac-specific Akt activation on aging-induced cardiac geometric and functional changes and underlying mechanisms involved. Cardiac geometry, contractile and intracellular Ca^{2+} properties were evaluated using echocardiography, edge-detection and fura-2 techniques. Level of insulin signaling and autophagy was evaluated by western blot. Our results revealed cardiac hypertrophy (enlarged chamber size, wall thickness, myocyte cross-sectional area), fibrosis, decreased cardiac contractility, prolonged relengthening along with compromised intracellular Ca^{2+} release and clearance in aged (24–26 month-old) mice compared with young (3–4 month-old) mice, the effects of which were accentuated by chronic Akt activation. Aging enhanced Akt and mTOR phosphorylation while reducing that of PTEN, AMPK and ACC with a more pronounced response in Akt transgenic mice. GSK3β phosphorylation and eNOS levels were unaffected by aging or Akt overexpression. Levels of beclin-1, Atg5 and LC3-II-to-LC3-I ratio were decreased in aged hearts, the effect of which with the exception of Atg 5 was exacerbated by Akt overactivation. Levels of p62 were significantly enhanced in aged mice with a more pronounced increase in Akt mice. Neither aging nor Akt altered β-glucuronidase activity and cathepsin B although aging reduced LAMP1 level. In addition, rapamycin reduced aging-induced cardiomyocyte contractile and intracellular Ca^{2+} dysfunction while Akt activation suppressed autophagy in young but not aged cardiomyocytes. In conclusion, our data suggest that Akt may accentuate aging-induced cardiac geometric and contractile defects through a loss of autophagic regulation.

Keywords Akt · Aging · Autophagy · Cardiac geometry · Contractile function · Insulin signaling

Y. Hua and Y. Zhang contributed equally.

Y. Hua · Y. Zhang · A. F. Ceylan-Isik · J. M. Nunn · J. Ren (✉)
Center for Cardiovascular Research and Alternative Medicine, University of Wyoming College of Health Sciences, Laramie, WY 82071, USA
e-mail: jren@uwyo.edu

Y. Zhang
Department of Cardiology, Xijing Hospital, Fourth Military Medical University, Xi'an 710032, China

L. E. Wold
The Department of Pediatrics, Center for Cardiovascular and Pulmonary Research, The Research Institute at Nationwide Children's Hospital, The Ohio State University, Columbus, OH 43205, USA

Introduction

Aging is a complicated pathophysiological process accompanied with a wide array of biological adaptations, including progressive myocardial remodeling and deteriorated cardiac reserve [6, 8, 36, 62]. Cardiac aging is usually characterized by increased left ventricular wall thickness and chamber size, changes in diastolic filling patterns such as prolonged diastolic duration, cardiac fibrosis and compromised ventricular contractile function, all of which contribute to the increasing incidence of cardiac morbidity and mortality in the elderly [36, 55, 62]. A number of theories have been proposed to be responsible for the

pathogenesis of the cardiac aging process such as myosin heavy chain isozyme switch, changes in gap junction structure, mitochondrial damage and free radical accumulation, leading to dysregulated intracellular Ca^{2+} homeostasis and excitation–contraction coupling [7, 36, 61, 62]. However, none of these speculations have been confirmed by clinical findings to explain the complex cardiac aging process. Although Akt is commonly recognized as an essential survival signaling molecule under cardiac stress such as ischemia–reperfusion injury [3, 9, 66], a recent report indicated that suppression of phosphoinositide 3-kinase (PI3K) may prevent aging-induced pathological changes in the heart [30]. This evidence has corroborated a role for PI3K and its downstream signaling targets including Akt in cardiac aging.

Autophagy, an evolutionarily conserved process of lysosome-dependent turnover of damaged proteins and organelles, plays a pivotal role in the maintenance of cellular environment in the heart [2, 47]. Autophagy is critical to cell survival, the interruption of which may initiate severe ventricular dysfunction, cardiomyopathy and ultimately heart failure [47, 63]. Although the precise role of autophagy in the regulation of biological responses and function is still unknown, loss of autophagy governed by mammalian target of rapamycin (mTOR) was demonstrated to accelerate aging [1, 27, 54, 56, 57]. In particular, reduced autophagy with aging has been speculated to be responsible for aging-associated buildup of damaged intracellular components such as protein aggregate lipofuscin, resulting in altered cellular homeostasis and loss of function in aging [12, 21, 56, 64]. Autophagy is potentially regulated by AMP-dependent protein kinase (AMPK), while being negatively regulated by mTOR through phosphorylation of its downstream targets such as p70s6k [20, 52]. TOR signaling has been considered as the main driver for aging since interrupted TOR signaling may extend lifespan [5, 25]. Given the critical role for Akt in the critical regulation of mTOR and cardiac geometry [10, 15, 23, 28], the present study was designed to examine the role of chronic Akt activation on aging-induced geometric, functional and intracellular Ca^{2+} homeostatic changes in the heart with a focus on autophagy. The Akt up- and downstream- signaling molecules including insulin receptor, phosphoinositide dependent kinase 1 (PDK1), mammalian target of rapamycin (mTOR), glycogen synthase kinase-3 β (GSK3β) and eNOS [19, 48] were examined in wild-type and Akt overexpression transgenic mice. In addition, Akt signaling is under the negative control of phosphatase and tensin homologue on chromosome ten (PTEN) to participate in the pathophysiology of a variety of diseases including myocardial hypertrophy, heart failure and preconditioning [48], therefore phosphorylation of PTEN was also scrutinized. Given that AMPK and Akt signaling are often inversely correlated such that Akt negatively regulates AMPK phosphorylation [34], AMPK and its substrate acetyl-CoA carboxylase (ACC) were evaluated. Recent evidence suggested an essential role for sequestosome-1 (SQSTM, also known as p62) as an autophagy adaptor in autophagosome formation and protein turnover [31]. Levels of p62 (total and triton-insoluble) were examined in young or aged mouse hearts. Given that autophagy quantification is heavily impacted by autophagic flux in particular lysosomal degradation [21], lysosomal activity was determined in young or aged mouse hearts using a β-glucuronidase activity assay [11, 33], as well as levels of cathepsin B and LAMP1, two key autophagy-related lysosomal proteins [17, 22].

Methods and materials

Cardiac-specific Akt overexpression mice and intraperitoneal glucose tolerance test (IPGTT)

All animal procedures were approved by the Animal Care and Use Committee at the University of Wyoming (Laramie, WY). Mice overexpressing the hemagglutinin (HA)-tagged Akt with src myristoylation signal under the direction of the murine α-myosin heavy-chain promoter were obtained from Dr. Anthony Rosenzweig at the Harvard Medical School (Boston, MA). The cardiac-specific Akt transgenic mice were genotyped using PCR [42]. Both 3–4 month-old (denoted as "young") and 24–26 month-old (as "old") male wild-type (WT) and Akt overexpression mice were maintained on a 12/12-light/dark cycle with free access to tap water until experimentation. At the time of sacrifice, blood glucose and plasma insulin levels were measured using a glucose monitor and an ELISA commercial kit, respectively. The homeostasis model assessment of insulin resistance (HOMA-IR) was used to estimate insulin resistance based on the following equation: fasting insulin $(\mu U/ml) \times$ fasting blood glucose $(mM)/22.5$ [44]. Prior to sacrifice, mice were fasted for 12 h and were then given an intraperitoneal (i.p.) injection of glucose (2 g/kg b.w.). Blood samples were drawn from the tail vein immediately prior to the glucose challenge, as well as 15, 30, 60 and 120 min thereafter. Blood glucose levels were determined using an Accu-Chek III glucose analyzer. The area under the curve (AUC) was calculated using trapezoidal analyses for each adjacent time point and serum glucose level.

Echocardiographic assessment

Cardiac geometry and function were evaluated in anesthetized (Avertin 2.5%, 10 μl/g, b.w., i.p.) mice using 2-D

guided M-mode echocardiography (Sonos 5500) equipped with a 15–6 MHz linear transducer. Left ventricular (LV) anterior and posterior wall dimensions during diastole and systole were recorded from three consecutive cycles in M-mode using method adopted by the American Society of Echocardiography [16]. Fractional shortening was calculated from LV end-diastolic (EDD) and end-systolic (ESD) diameters using the equation $(EDD - ESD)/EDD$. Heart rates were averaged over 10 cycles.

Isolation of mouse cardiomyocytes

Hearts were rapidly removed from anesthetized mice and mounted onto a temperature-controlled (37°C) Langendorff system. Following perfusion with a modified Tyrode's solution (Ca^{2+} free) for 2 min, the heart was digested with a Ca^{2+}-free KHB buffer containing liberase blendzyme 4 (Hoffmann-La Roche Inc., Indianapolis, IN) for 20 min. The modified Tyrode solution (pH 7.4) contained the following (in mM): NaCl 135, KCl 4.0, $MgCl_2$ 1.0, HEPES 10, NaH_2PO4 0.33, glucose 10, butanedione monoxime 10, and the solution was gassed with 5% CO_2–95% O_2. The digested heart was then removed from the cannula and the left ventricle was cut into small pieces in the modified Tyrode's solution. Tissue pieces were gently agitated and the pellet of cells was resuspended. Extracellular Ca^{2+} was added incrementally back to 1.20 mM over 30 min. A yield of at least 60–70% viable rod-shaped cardiomyocytes with clear sacromere striations was achieved. Only rod-shaped myocytes with clear edges were selected for contractile and intracellular Ca^{2+} studies [16].

Cell shortening/relengthening

Mechanical properties of cardiomyocytes were assessed using a SoftEdge MyoCam® system (IonOptix Corporation, Milton, MA) [16]. In brief, cells were placed in a Warner chamber mounted on the stage of an inverted microscope (Olympus, IX-70) and superfused (1 ml/min at 25°C) with a buffer containing (in mM): 131 NaCl, 4 KCl, 1 $CaCl_2$, 1 $MgCl_2$, 10 glucose, 10 HEPES, at pH 7.4. The cells were field stimulated with a supra-threshold voltage at a frequency of 0.5 Hz (unless otherwise stated), 3 ms duration, using a pair of platinum wires placed on opposite sides of the chamber connected to a FHC stimulator (Brunswick, NE). The myocyte being studied was displayed on the computer monitor using an IonOptix MyoCam camera. IonOptix SoftEdge software was used to capture changes in cell length during shortening and relengthening. Cell shortening and relengthening were assessed using the following indices: peak shortening (PS)—peak ventricular contractility, time-to-PS (TPS)—contraction duration, and time-to-90% relengthening (TR_{90})—cardiomyocyte relaxation duration, maximal velocities of shortening (+dL/dt) and relengthening (−dL/dt)—maximal velocities of ventricular pressure rise/fall. In the case of altering stimulus frequency from 0.1 to 5.0 Hz, the steady state contraction of the myocyte was achieved (usually after the first 5–6 beats) before PS was recorded.

Intracellular Ca^{2+} transient measurement

Myocytes were loaded with fura-2/AM (0.5 μM) for 10 min and fluorescence measurements were recorded with a dual-excitation fluorescence photomultiplier system (IonOptix). Cardiomyocytes were placed on an Olympus IX-70 inverted microscope and imaged through a Fluor 40× oil objective. Cells were exposed to light emitted by a 75 W lamp and passed through either a 360 or a 380 nm filter, while being stimulated to contract at 0.5 Hz. Fluorescence emissions were detected between 480 and 520 nm by a photomultiplier tube after first illuminating the cells at 360 nm for 0.5 s then at 380 nm for the duration of the recording protocol (333 Hz sampling rate). The 360 nm excitation scan was repeated at the end of the protocol and qualitative changes in intracellular Ca^{2+} concentration were inferred from the ratio of fura-2 fluorescence intensity (FFI) at the two wavelengths (360/380). Fluorescence decay time was measured as an indication of the intracellular Ca^{2+} clearing rate. Both single and bi-exponential curve fit programs were applied to calculate the intracellular Ca^{2+} decay constant [16].

Glucose uptake assay

Cardiomyocytes were washed 3 times with Krebs–Ringer-*N*-[2-hydro-ethyl]-piperazine-*N*′-[2-ethanesulfonic acid] (HEPES) (KRH, 136 mM NaCl, 4.7 mM KCl, 1.25 mM $CaCl_2$, 1.25 mM $MgSO_4$, 10 mM HEPES, pH 7.4) buffer and incubated with 2 ml KRH buffer at 37°C for 30 min. A cohort of cardiomyocytes from each group was subjected to insulin stimulation (10 nM, 15 min). Glucose uptake was initiated with addition of 0.1 ml KRH buffer and 2-deoxy-D-[3H] glucose (0.2 μ Ci/ml with a specific activity of 10 Ci/mmol) and 5 mM glucose. Glucose uptake was terminated after 30 min by washing the cells with cold PBS [13]. The cells were lysed overnight with 0.5 ml 0.5 M NaOH and 0.1% SDS (w/v). Radioactivity retained by the cell lysates was determined using a scintillation counter (1 cpm = 0.888×10^{-12} Ci, Beckmann LC 6000IC) and normalized to protein concentration measured using a Bradford Protein Assay Kit. All assays were repeated in duplicate to ensure reproducibility of the results. Data from 5–6 mice per group were used for final data analyses.

Histological examination

Following anesthesia, hearts were arrested in diastole with saturated KCl, excised and fixed in 10% neutral-buffered formalin at room temperature for 24 h. The specimen was processed through graded alcohol concentrations, cleared in xylene, embedded in paraffin, and serial sections were cut at 5 μm and stained with hematoxylin and eosin (H&E). Frozen hearts were used for Masson's Trichrome staining. Serial sections were cut at 10 μm thickness using a Leica, cryomicrotome (Model CM3050S, Leica Microsystems, Buffalo Grove, IL, USA) prior to fixation in 4% paraformaldehyde for 30 min. Following two washes with phosphate buffered saline (PBS), the sections were stained with a Trichrome stain kit (Sigma-Aldrich, St. Louis, MO, USA). Cardiomyocyte cross-sectional area and fibrosis-to-total area ratio were measured from cardiomyocytes with clear myofiber outlines on a digital microscope (400×) using the Image J (version1.34S) software [16].

Lipofuscin assay

Frozen heart tissues were homogenized in chloroform–methanol (1:20, w:v). The chloroform-rich layer was mixed with methanol following 15 min centrifugation at 15,000*g*. Fluorescence in the sample was measured at an excitation wavelength of 350 nm and emission wavelength of 485 nm using a spectrofluorimeter (Molecular Devices, SpectraMAX Gemini XS, CA, USA) [53]. The data were expressed as fluorescence intensity per 100 mg tissue.

β-glucuronidase assay

Subcellular fractions were separated. Briefly, a portion of the heart was homogenized in an ice-cold 0.25 M sucrose solution. The homogenate was centrifuged at 600*g* for 10 min at 4°C. The supernatant was further centrifuged at 16,000*g* for 30 min at 4°C. The sediment (lysosomal fraction) was collected and incubated with an ice-cold lysis buffer for 15 min prior to the determination of β-glucuronidase activity. Activity was determined according to the method of Koldovasky [11, 33]. The assay mixture contained 0.5 ml of freshly prepared 4 mM *p*-nitrophenyl β-D-glucuronide (final concentration of 2 mM) in 0.1 M sodium acetate buffer (pH 5.0). Twenty-five microlitre of lysosome lyses was made up to 1.0 ml with assay buffer and incubated at 37°C for 1 h. The reaction was stopped by the addition of 3 ml of 0.2 M glycine–NaOH buffer (pH 11.7). Absorbance was measured at 410 nm using a spectrophotometer (Molecular Devices Spectra Max 190, CA, USA). The data were expressed as μmol *p*-nitrophenol liberated per hour per 100 mg protein.

Western blot analysis

Murine heart tissues were homogenized and sonicated in a lysis buffer containing 20 mM Tris (pH 7.4), 150 mM NaCl, 1 mM EDTA, 1 mM EGTA, 1% Triton, 0.1% sodium dodecyl sulfate (SDS), and a protease inhibitor cocktail (Thermo Scientific). Protein levels of insulin receptor β, phosphorylated PDK1 (pPDK1,Ser^{241}), Akt, phosphorylated Akt (pAkt) at both Ser^{473} and Thr^{308}, GSK3β, phosphorylated GSK3β (pGSK3β, Ser^{9}), PTEN, phosphorylated PTEN (pPTEN, Ser^{380}), AMPK, phosphorylated AMPK (pAMPK, Thr^{172}), acetyl CoA Carboxylase (ACC), phosphorylated ACC (pACC, Ser^{79}), eNOS, mTOR, phosphorylated mTOR (pmTOR, Ser^{2448}), Beclin 1, Atg5, LC3 isoform, p62, cathepsin B and LAMP1 were examined using standard western immunoblotting. All antibodies were obtained from Cell Signaling Technology (Beverly, MA, USA) except p62 antibody (PROGEN Biotechnik, Heidelberg, Germany) and cathepsin B antibody (Sigma-Aldrich, St. Louis, MO, USA). Membranes were probed with respective antibodies using α-tubulin serving as the loading control. To detect the expression of cellular triton-insoluble p62, cellular proteins were separated into detergent-soluble and -insoluble fractions with the 2% Triton X-100 buffer (50 mM Tris (pH 8.0), 150 mM NaCl, 1 mM EDTA, 10% glycerol, 2% Triton X-100, protein inhibitor cocktail). Buffer with 1% SDS was used to solve the insoluble fractions. The triton-insoluble fractions were subjected to western blot analysis and probed with p62 and lamin A/C (loading control, Cell Signaling Technology) antibodies [18]. The membranes were incubated with horseradish peroxidase (HRP)-coupled secondary antibodies. Following immunoblotting, the film was scanned and detected using a Bio-Rad Calibrated Densitometer and the intensity of the immunoblot bands was normalized to that of α-tubulin or lamin A/C (for insoluble p62) [16].

Data analyses

Data were expressed as Mean ± SEM. Statistical significance ($p < 0.05$) was estimated using one-way analysis of variation (ANOVA) or repeated-measures of ANOVA (for Fig. 1) followed by a Tukey's test for post hoc analysis. The number of replicates for each experiment is expressed in the figure legends.

Results

General biometric and echocardiographic characteristics

The biometric profiles of young or old WT and Akt over-expression mice are shown in Table 1. Cardiac

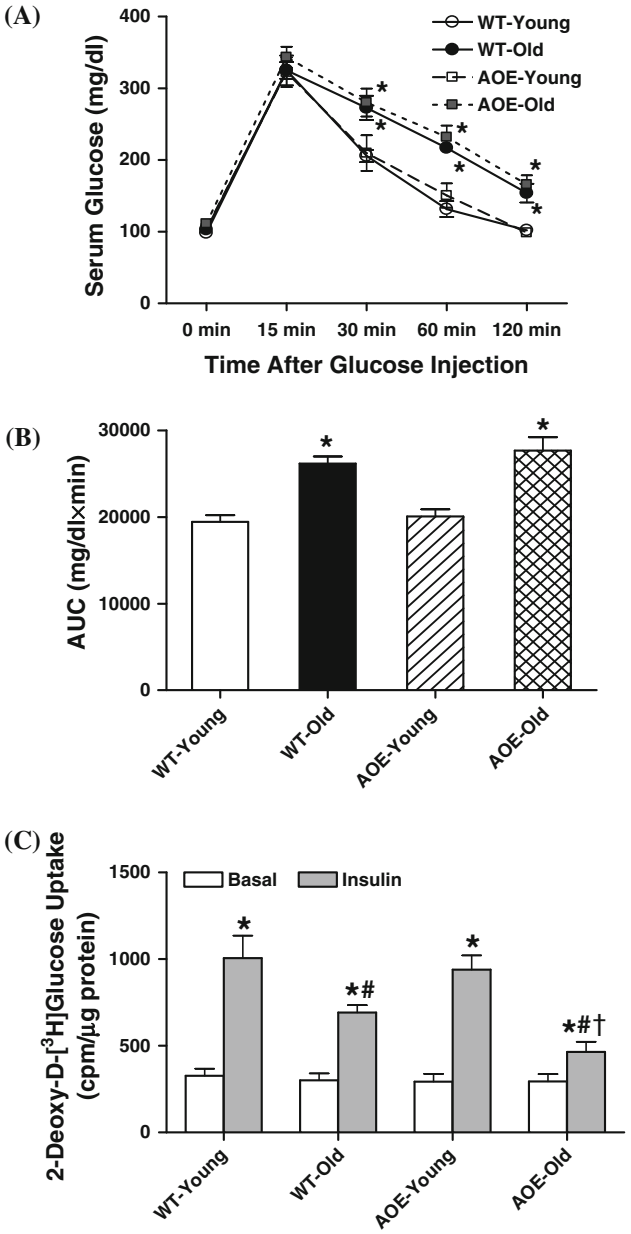

Fig. 1 Intraperitoneal glucose tolerance test (IPGTT, 2 g/kg) and glucose uptake in WT and Akt overexpression (AOE) mice at young and old ages. **a** Serum glucose levels within 120 min following IPGTT challenge, **b** area underneath the curve (AUC), **c** 2-Deoxyglucose uptake in freshly isolated cardiomyocytes from WT and AOE mice with or without insulin treatment (100 nm, 15 min). Mean ± SEM, $n = 5$–6 mice or isolations per group, $^{*}p < 0.05$ versus respective WT-young or basal group, $^{\#}p < 0.05$ versus insulin-treated WT-young group, $^{\dagger}p < 0.05$ versus respective WT-old group

overexpression of Akt did not elicit any notable effect on body weight compared with the age-matched WT mice. Although Akt activation failed to affect heart weight at the young age, it prompted overt cardiac hypertrophy (both absolute weight and size) in aged mice. Aged WT and Akt transgenic mice displayed greater body and heart weights (and heart size in Akt mice) compared with their young counterparts. Neither aging nor Akt activation or the combination of the two significantly altered fasting blood glucose levels. Aging, but not Akt overexpression, increased plasma insulin and HOMA-IR levels. Aging but not Akt activation significantly increased left ventricular wall thickness and ESD, the effects of which were more pronounced in Akt mice. Neither aging nor Akt overexpression significantly affected EDD and fractional shortening, although the combination of the two overtly increased EDD while decreasing fractional shortening. Heart rate was unaffected by either aging or Akt overexpression.

IPGTT and glucose uptake in young or old WT and Akt overexpression mice

Following acute intraperitoneal glucose challenge, changes in serum glucose levels of the young WT and Akt mice displayed similar patterns, i.e., peaking at 15 min and returning to near baseline after 120 min. However, the post-challenge glucose levels remained at significantly higher levels between 15 and 120 min for both aged groups, indicating glucose intolerance. The basal fasting glucose levels were comparable among all groups, excluding the existence of full-blown diabetes (Fig. 1a). These findings were supported by the area under the IPGTT curve (AUC) where elevated AUC levels were observed in both old mouse groups with little effect of Akt overactivation at the young age (Fig. 1b). Measurement of 2-deoxy-D-[^{3}H] glucose uptake revealed that neither aging nor Akt overexpression (or both) affected basal glucose uptake. Acute insulin challenge (100 nm) significantly stimulated glucose uptake, in a similar manner, in the young WT and Akt transgenic mice. Aging drastically abrogated insulin-stimulated glucose uptake with a more pronounced decrease in cardiomyocytes from Akt mice (Fig. 1c).

Cardiomyocyte contractile and intracellular Ca^{2+} transient properties

Aging, but not Akt overactivation, significantly elongated resting cardiomyocyte length. Aging significantly reduced peak shortening, maximal velocities of shortening/relengthening (±dL/dt) and prolonged time-to-90% relengthening (TR_{90}) without affecting time-to-peak shortening (TPS). While Akt overexpression itself did not elicit any significant effects on the mechanical parameters of young mice, it significantly accentuated aging-induced alterations in PS, ±dL/dt and TR_{90} without affecting TPS (Fig. 2). To explore the possible mechanisms of action between aging and Akt overexpression, intracellular Ca^{2+} handling was evaluated using fura-2 fluorescence techniques. Our data revealed that neither aging nor Akt overexpression significantly affected resting intracellular Ca^{2+} levels, although the

Table 1 Biometric and echocardiographic parameters of WT and AOE mice at young and old age

Parameter	WT-young	WT-old	AOE-young	AOE-old
Body weight (g)	22.2 ± 0.6	30.1 ± 0.8*	22.0 ± 0.5	29.3 ± 0.8*
Heart weight (mg)	120 ± 3	157 ± 5*	123 ± 2	184 ± 4*,#
Heart/body weight (mg/g)	5.41 ± 0.08	5.24 ± 0.19	5.58 ± 0.08	6.30 ± 0.21*,#
Fasting blood glucose (mg/dl)	99 ± 2	97 ± 4	101 ± 5	113 ± 9
Plasma insulin (ng/ml)	0.41 ± 0.07	2.18 ± 0.41*	0.44 ± 0.08	2.33 ± 0.30*
HOMA-IR (mmol/l*μU/ml)	2.40 ± 0.39	12.22 ± 1.96*	2.63 ± 0.41	14.87 ± 2.28*
Heart rate (bpm)	423 ± 9	520 ± 49	450 ± 10	472 ± 20
Wall thickness (mm)	0.64 ± 0.06	1.24 ± 0.08*	0.64 ± 0.04	1.45 ± 0.03*,#
EDD (mm)	2.88 ± 0.36	3.24 ± 0.19	2.88 ± 0.05	3.53 ± 0.07*,#
ESD (mm)	1.59 ± 0.15	1.89 ± 0.10*	1.56 ± 0.04	2.19 ± 0.04*,#
Fractional shortening (%)	43.8 ± 3.1	41.6 ± 0.7	45.7 ± 1.5	37.9 ± 0.8*,#

HW heart weight, *HOMA-IR* homeostatic model assessment of insulin resistance, *EDD* end diastolic diameter, *ESD* end systolic diameter, *LV* left ventricular

Mean ± SEM, $n = 6$–7 mice per group

* $p < 0.05$ versus WT-young group, # $p < 0.05$ versus WT-old group

combination of the two overtly elevated resting intracellular Ca^{2+} levels. Aging, but not Akt overactivation, itself significantly decreased the electrically stimulated rise in intracellular Ca^{2+} (ΔFFI) and intracellular Ca^{2+} clearance rate (either single or bi-exponential) with a more pronounced response in Akt mice (Fig. 3a–d).

Effect of increased stimulation frequency on cardiomyocyte shortening amplitude

Mouse hearts normally contract at very high frequencies (>400), whereas our recordings were performed at 0.5 Hz. To evaluate the impact of aging and/or Akt overexpression on cardiac contractile function under higher frequencies, we increased stimulus frequency up to 5.0 Hz (300 beats/min) and recorded the steady-state PS amplitude. Cardiomyocytes were initially stimulated to contract at 0.5 Hz for 5 min to ensure steady-state prior to commencing the frequency response. Figure 3e displays a negative staircase of PS with increased stimulus frequency in all four groups with a steeper decline in the aged mice. Although Akt overexpression itself failed to elicit any obvious effects on the patterns of frequency-shortening response, it exacerbates aging-induced decline in PS amplitude. These data favor a possible role for reduced intracellular Ca^{2+} cycling and stress intolerance in Akt overactivation-exacerbated mechanical anomalies during aging.

Effect of Akt overexpression and aging on myocardial histology

To assess the impact of Akt activation on myocardial histology in aging, cardiomyocyte cross-sectional area and cardiac fibrosis were examined. H&E staining revealed an increased cardiomyocyte transverse cross-sectional area in aged mouse hearts, consistent with increased left ventricular geometry (wall thickness and ESD) and heart weights in old WT mice. While Akt overexpression itself failed to affect cardiomyocyte cross-sectional area early on, it significantly accentuated aging-induced increase in cardiomyocyte cross-sectional area, again in line with the geometric and biometric findings. Masson's trichrome staining revealed enhanced cardiac fibrosis in aged mouse hearts. Importantly, while Akt activation itself did not affect cardiac fibrosis at the young age, it remarkably exacerbated aging-induced cardiac fibrosis (Fig. 4).

Effect of aging and Akt overexpression on insulin signaling

To elucidate the possible mechanisms of action behind aging and/or Akt overexpression-induced cardiac mechanical and intracellular Ca^{2+} derangements, molecules involved in insulin signaling were examined. Our data depicted that aging significantly upregulated insulin receptor β levels in WT but not Akt transgenic mice. Akt activation itself did not affect insulin receptor β levels. Levels of Akt were elevated in a comparable manner in young and aged Akt mice. Akt overexpression but not aging significantly enhanced PDK1 and Akt (Thr^{308}) phosphorylation with no synergistic effects. Aging and Akt overexpression significantly stimulated phosphorylation of Akt (Ser^{473}) and decreased PTEN phosphorylation with a more pronounced effect in aged Akt mice. Neither aging nor Akt overexpression significantly affected protein expression of PDK1, GSK3β and PTEN or GSK3β

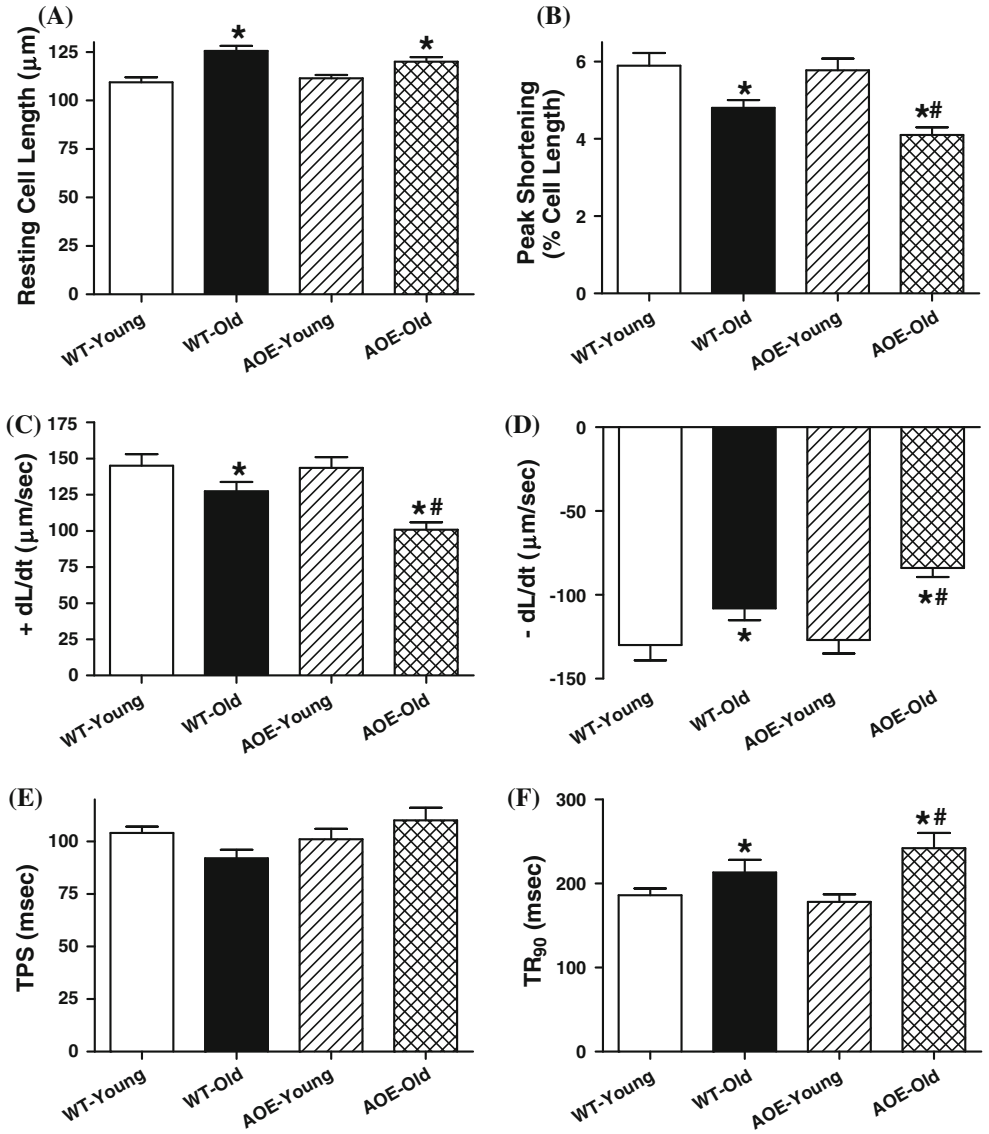

Fig. 2 Cardiomyocyte mechanical function in young or old WT and Akt overexpression (AOE) mice. **a** Resting cell length, **b** peak shortening (PS, normalized to resting cell length), **c** maximal velocity of shortening (+dL/dt), **d** maximal velocity of relengthening (−dL/dt), **e**: time-to-PS (TPS); and **f** time-to-90% relengthening (TR_{90}). Mean ± SEM, $n = 95$–96 cells from 5 mice per group, $^{*}p < 0.05$ versus WT-young group, $^{\#}p < 0.05$ versus WT-old group

phosphorylation. Aging itself did not overtly affect the expression of Akt (Fig. 5).

Effect of aging and Akt activation on AMPK, ACC, eNOS, mTOR, autophagy and lipofuscin

To further elucidate the signaling mechanisms involved in aging and/or Akt overexpression -induced myocardial dysfunction, western blotting was performed on signaling molecules including AMPK, the AMPK phosphorylation target ACC, eNOS, the Akt downstream signal mTOR and autophagic protein markers. Both aging and Akt overactivation significantly suppressed AMPK phosphorylation with a more pronounced inhibition in aged Akt mice. Likewise, both aging and Akt overexpression suppressed ACC phosphorylation with little additive effects between the two. Both aging and Akt overexpression facilitated mTOR phosphorylation with a more obvious increase in aged Akt mice. Neither aging nor Akt overexpression altered eNOS expression. Expression of pan AMPK, ACC and mTOR was unaffected by either aging or Akt overexpression, or a combination of both (Fig. 6). To evaluate the role of autophagy in aging and Akt overexpression-elicited cardiac geometric, function and intracellular Ca^{2+} handling responses, autophagic markers including Beclin-1, LC3-I/II, and Atg5 were examined and our results shown

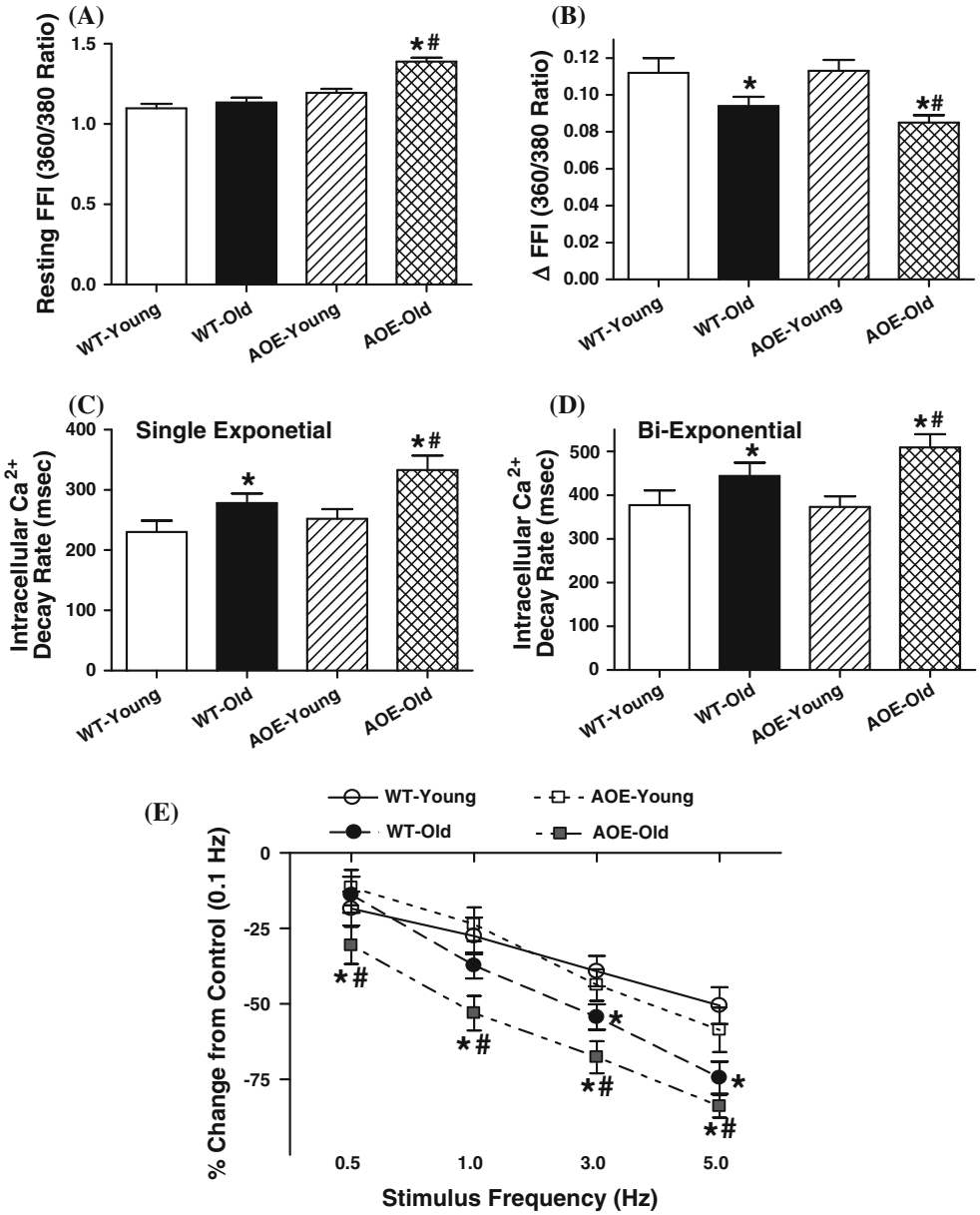

Fig. 3 Intracellular Ca^{2+} transient and frequency response in cardiomyocytes from young or old WT and Akt overexpression (AOE) mice. **a** Resting fura-2 fluorescence intensity (FFI), **b** electrically stimulated rise in FFI (ΔFFI), **c** single exponential intracellular Ca^{2+} decay, **d** bi-exponential intracellular Ca^{2+} decay, and **e** changes in peak shortening amplitude of cardiomyocytes (normalized to that obtained at 0.1 Hz from the same cell) at various stimulus frequencies (0.1–5.0 Hz). Mean ± SEM, $n = 82$ cells (*panels a–d*) and 23–26 cells (*panel e*) from 5 mice per group, $^{*}p < 0.05$ versus WT-young group, $^{\#}p < 0.05$ versus WT-old group

in Fig. 7 depicted overtly reduced autophagy in aging WT mice as evidenced by downregulated Beclin-1, Atg5, LC3-II levels and decreased LC3-II-to-LC3-I ratio. Akt overexpression itself did not exert any notable effects on autophagic protein markers, although it accentuated aging-induced decreases in Beclin-1, LC3-II and LC3-II-to-LC3-I ratio but not that of Atg5. Neither aging nor Akt overexpression affected the expression of LC3-I. Lastly, aged WT and Akt transgenic mice exhibited overtly elevated levels of protein aggregate lipofuscin, a protein aggregate marker for aging and oxidative stress [14], in a comparable manner within the heart. Akt activation itself did not elicit any effects on lipofuscin content at the young age.

Effects of aging and Akt overexpression on autophagy adaptor p62, β-glucuronidase activity as well as expression of cathepsin B and LAMP1

Recent evidence suggested that LC3 directly interacts with p62, a protein involved in autophagosome formation and

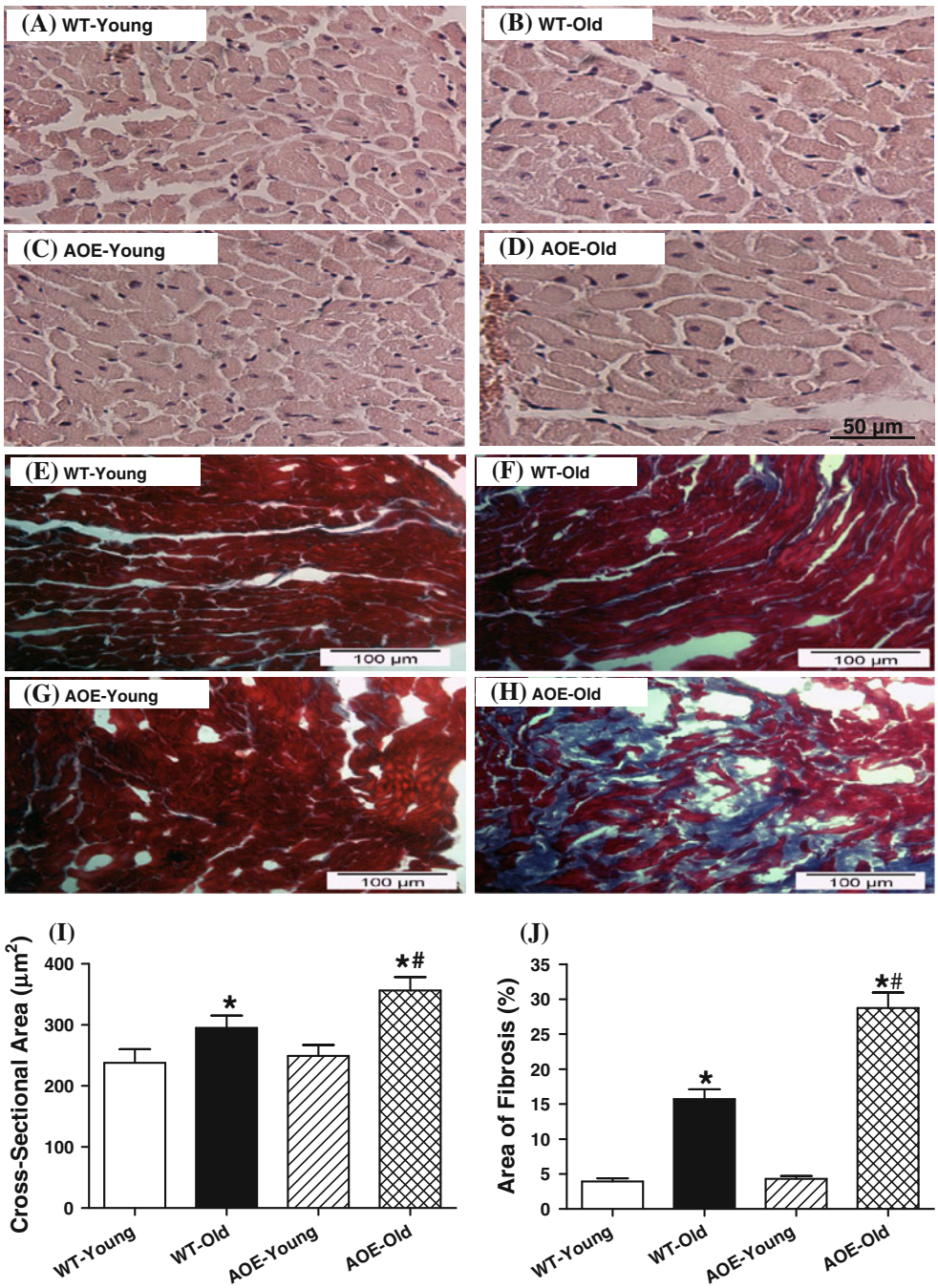

Fig. 4 Histological analyses of hearts from young or old WT and Akt overexpression (AOE) mice. **a–d** Representative H&E staining micrographs displaying transverse myocardial sections (×400), **e–h** representative Masson's Trichrome staining micrographs showing sections of left ventricular myocardiums (×200), **i** quantitative analyses of cardiomyocyte cross-sectional (transverse) area using measurements of ~100 cells from 3 to 4 mice per group, and **j** quantitative analyses of fibrotic area (Masson's trichrome stained area in light blue color normalized to the total myocardial area) from ~100 sections from 4 mice per group. Mean ± SEM, $^{*}p < 0.05$ versus WT-young group, $^{\#}p < 0.05$ versus WT-old group

protein turnover [31]. Total and triton-insoluble p62 were evaluated in young or aged WT and Akt transgenic mice. Neither age nor Akt overactivation affected the level of total p62, although the combination of the two upregulated total p62 levels. Aging, but not Akt overactivation, enhanced triton-insoluble p62 levels, with a more pronounced rise in aged Akt transgenic mice (Fig. 8). To determine whether aging or Akt-induced effects on autophagy was associated with change in lysosomal activity, β-glucuronidase activity, which is usually used as

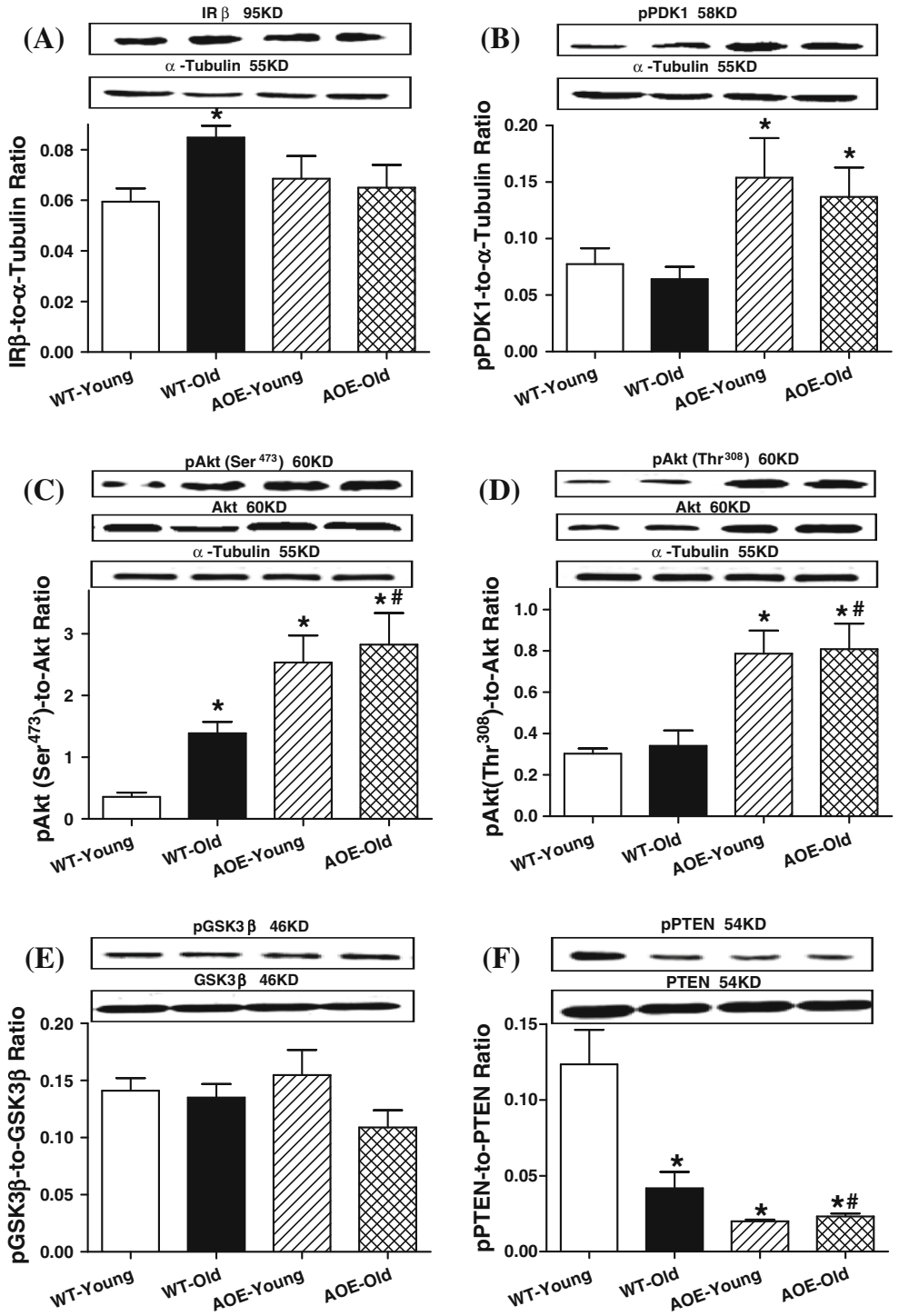

Fig. 5 Effect of Akt overexpression (AOE) on aging-induced change in insulin receptor β (*panel a*), PDK1 phosphorylation (*panel b*), Akt phosphorylation (pAkt-to-Akt ratio) at Ser^{473} (*panel c*) and Thr^{308} (*panel d*), GSK3β phosphorylation (pGSK3β-to-GSK3β ratio, *panel e*), and PTEN phosphorylation (pPTEN-to-PTEN ratio, *panel f*). Insets: representative gel blots depicting expression and phosphorylation of these proteins using specific antibodies. α-Tubulin was used as the loading control. Mean ± SEM, $n = 5$–7 mice per group, $^{*}p < 0.05$ versus WT-young group, $^{\#}p < 0.05$ versus WT-old group

an index for lysosomal activity [11, 33], was determined in young or aged WT and Akt transgenic mice. Our data failed to revealed altered β-glucuronidase activity in response to aging, Akt overactivation, or both. In addition, the levels of the two autophagy-related lysosomal proteins, cathepsin B and LAMP1, were examined [17, 22]. Neither

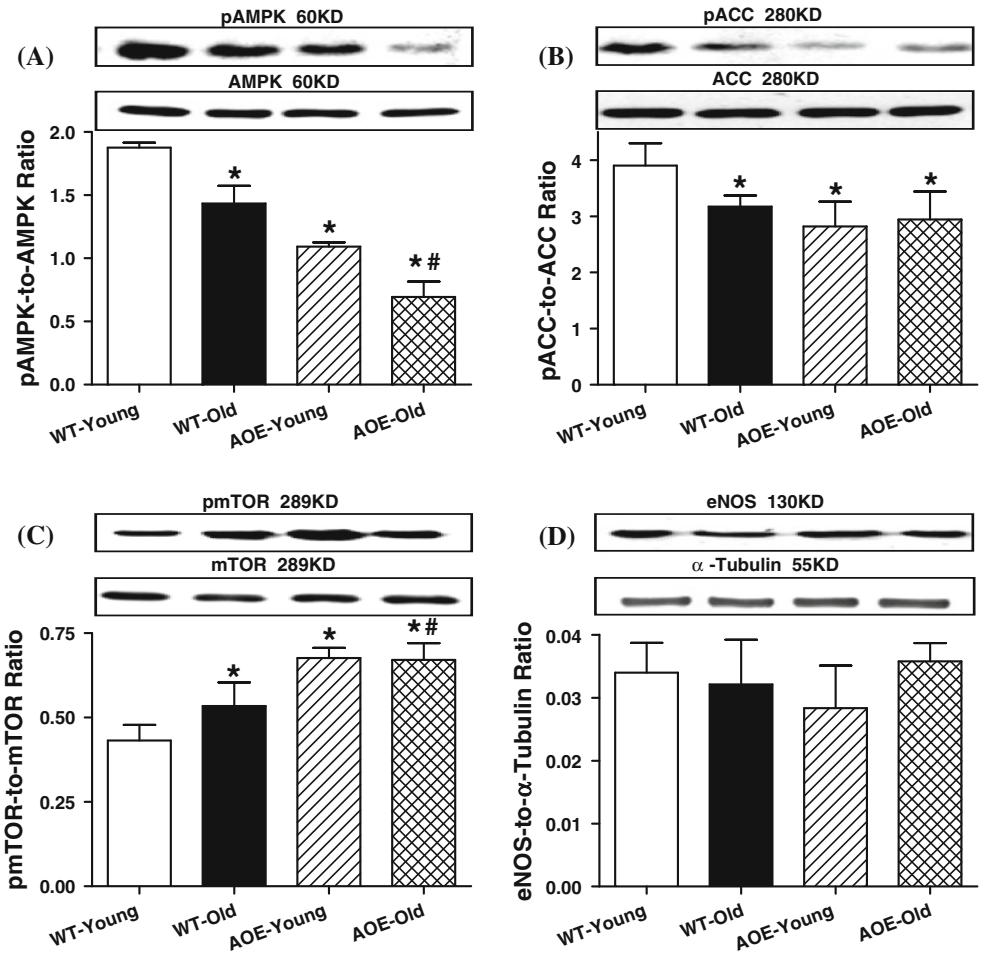

Fig. 6 Effect of Akt overexpression (AOE) on aging-induced change in AMPK phosphorylation (pAMPK-to-AMPK ratio, *panel a*), ACC phosphorylation (pACC-to-ACC ratio, *panel b*), mTOR phosphorylation (pmTOR-to-mTOR ratio, *panel c*), and eNOS expression (*panel d*). Insets: representative gel blots of these proteins using specific antibodies. α-Tubulin was used as the loading control. Mean ± SEM, $n = 5$–6 mice per group, $^{*}p < 0.05$ versus WT-young group, $^{\#}p < 0.05$ versus WT-old group

aging nor Akt overexpression significantly affected cathepsin B expression with no synergistic effects between the two. Aging significantly downregulated the levels of LAMP1 in WT but not the Akt transgenic group. Lastly, Akt overactivation itself did not affect LAMP1 level.

Effects of the autophagy inducer rapamycin on cardiomyocyte contractile and intracellular Ca^{2+} derangement in aging

To further examine the role of autophagy in aging-induced cardiac contractile alterations, cardiomyocytes from both young and aged male WT mice were treated with rapamycin, an autophagy inducer which is capable of eliciting autophagy within 1–2 h [24, 50]. While rapamycin (5 μM for 4 h) failed to elicit any mechanical responses in young mice, it significantly alleviated or abrogated aging-induced cardiomyocyte contractile defects including reduced PS and ±dL/dt, shortened TPS and prolonged TR_{90}. Aged murine cardiomyocytes possessed a lower LC3-II-to-LC3-I ratio compared with cardiomyocytes from young mice, depicting a lower autophagic capacity. Furthermore, pepstatin A, a lysosome proteinase inhibitor [41], provoked an increase in the LC3II-to-LC3I ratio in cardiomyocytes from both young and old mice. These data did not favor a major role for lysosomal enzymatic activity in aging-associated loss of autophagy. Acute treatment with insulin (100 nm), an Akt activator, suppressed autophagy as evidenced by a reduced LC3-II-to-LC3-I ratio in the young but not old murine cardiomyocytes. To the contrary, rapamycin significantly facilitated autophagy (shown as elevated LC3-II-to-LC3-I ratios) in cardiomyocytes from both age groups (Fig. 9). To further examine if intracellular Ca^{2+} handling plays a role in autophagy-regulated cardiomyocyte function in aging, fura-2 fluorescence was evaluated in cardiomyocytes from young and aged WT

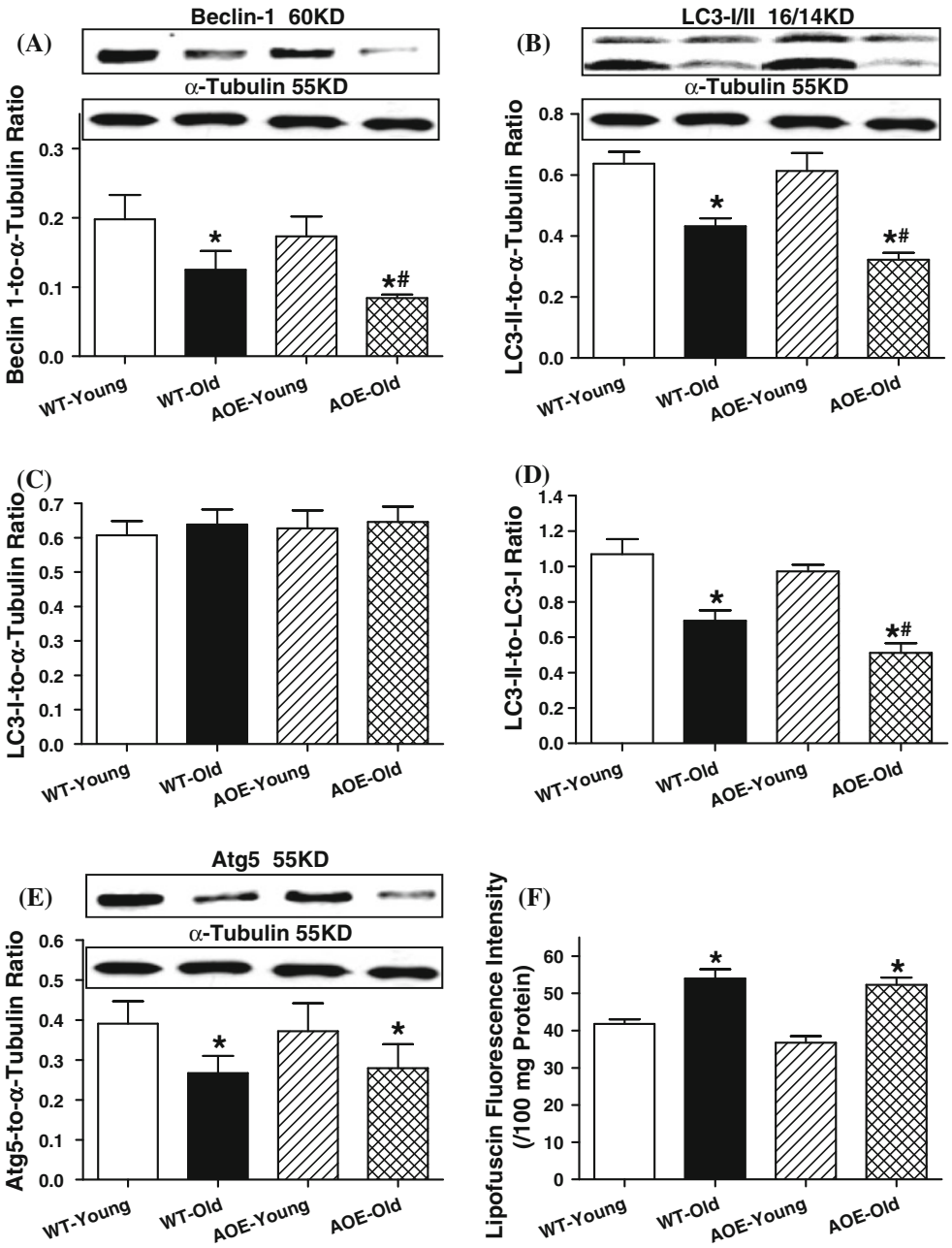

Fig. 7 Effect of Akt overexpression (AOE) on aging-induced change in autophagic and aging markers. **a** Beclin-1 expression, **b** LC3-II expression, **c** LC3-I expression, **d** LC3-II-to-LC3-I ratio, **e** Atg5 expression, and **f** lipofuscin levels. Insets: representative gel blots of the autophagic markers Beclin-1, LC3-1/II, Atg5 and α-tubulin (loading control) using specific antibodies; Mean ± SEM, $n = 5$–8 mice per group, $^{*}p < 0.05$ versus WT-young group, $^{\#}p < 0.05$ versus WT-old group

mice following incubation with rapamycin (5 μM for 4 h). Our data presented in Fig. 10 revealed that rapamycin abrogated aging-induced cardiomyocyte intracellular Ca^{2+} mishandling including reduced ΔFFI and prolonged intracellular Ca^{2+} clearance. Rapamycin itself did not elicit any notable intracellular Ca^{2+} response in young mice. These data support a beneficial role for autophagic induction against aging-induced cardiac contractile and intracellular Ca^{2+} defects.

Discussion

Our study revealed that chronic activation of Akt accentuated aging-associated cardiac hypertrophy, interstitial fibrosis, contractile dysfunction, and intracellular Ca^{2+} mishandling. Akt overexpression significantly worsened the aging-induced loss of insulin sensitivity in the heart along with suppressed autophagy including buildup of insoluble p62, favoring a role for Akt-mediated autophagy

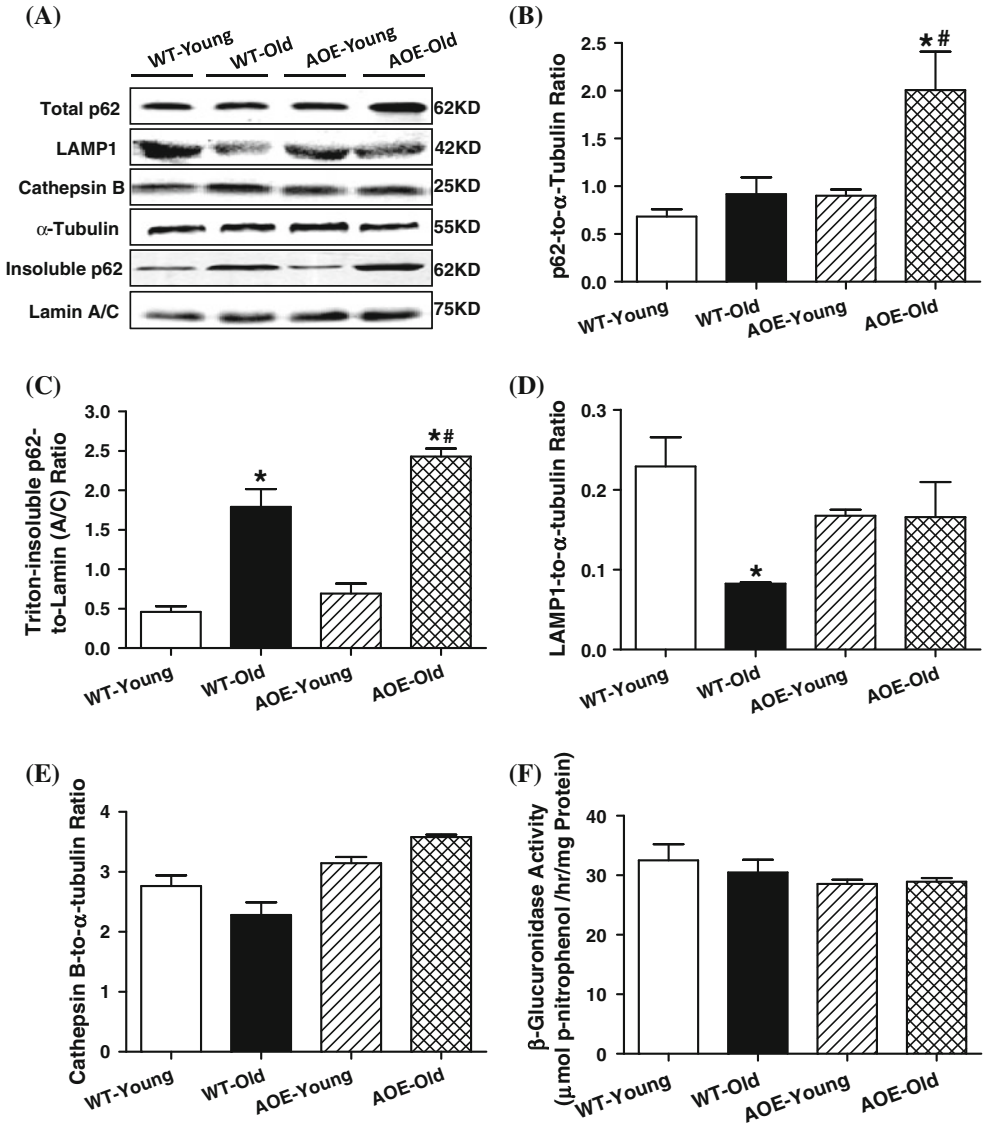

Fig. 8 Effect of Akt overexpression (AOE) on aging-induced change in the autophagic adapter p62 and lysosomal enzymes. **a** Representative gel blots of total and insoluble p62, LAMP1, cathepsin B and α-tubulin (loading control, Lamin a/c was used as loading control for insoluble p62) using specific antibodies, **b** total p62 expression, **c** triton-insoluble p62 expression, **d** LAMP1 expression, **e** cathepsin B expression and **f** lysosomal enzyme *β*-glucuronidase activity. Mean ± SEM, $n = 5$–8 mice per group, $^{*}p < 0.05$ versus WT-young group, $^{\#}p < 0.05$ versus WT-old group

regulation in Akt activation-accentuated cardiac aging. Reduced autophagy or inability to remove damaged structures was supported by the accumulation of garbage protein aggregate such as lipofuscin, an aging marker [14]. The involvement of autophagy in cardiac aging was further substantiated by in vitro autophagy induction where rapamycin alleviated aging-induced cardiomyocyte mechanical and intracellular Ca^{2+} derangements. These results collectively suggest a possible role for Akt and autophagy in the regulation of myocardial morphology and function in the aging process and more importantly, the therapeutic potential for autophagy in cardiac aging.

Akt activation worsens cardiac geometry, contractile and intracellular Ca^{2+} properties in aging

Changes in myocardial morphology, geometry and contractile function are typical in aged hearts characterized by a buildup of the protein aggregate lipofuscin, cardiac hypertrophy, interstitial fibrosis, intracellular Ca^{2+} defect, and compromised contractility in particular prolonged diastolic duration [14, 21, 35, 61, 62]. However, ventricular ejection fraction, the essential measure of left ventricular systolic performance, is usually preserved during aging, potentially due to enlarged ventricular end diastolic volume

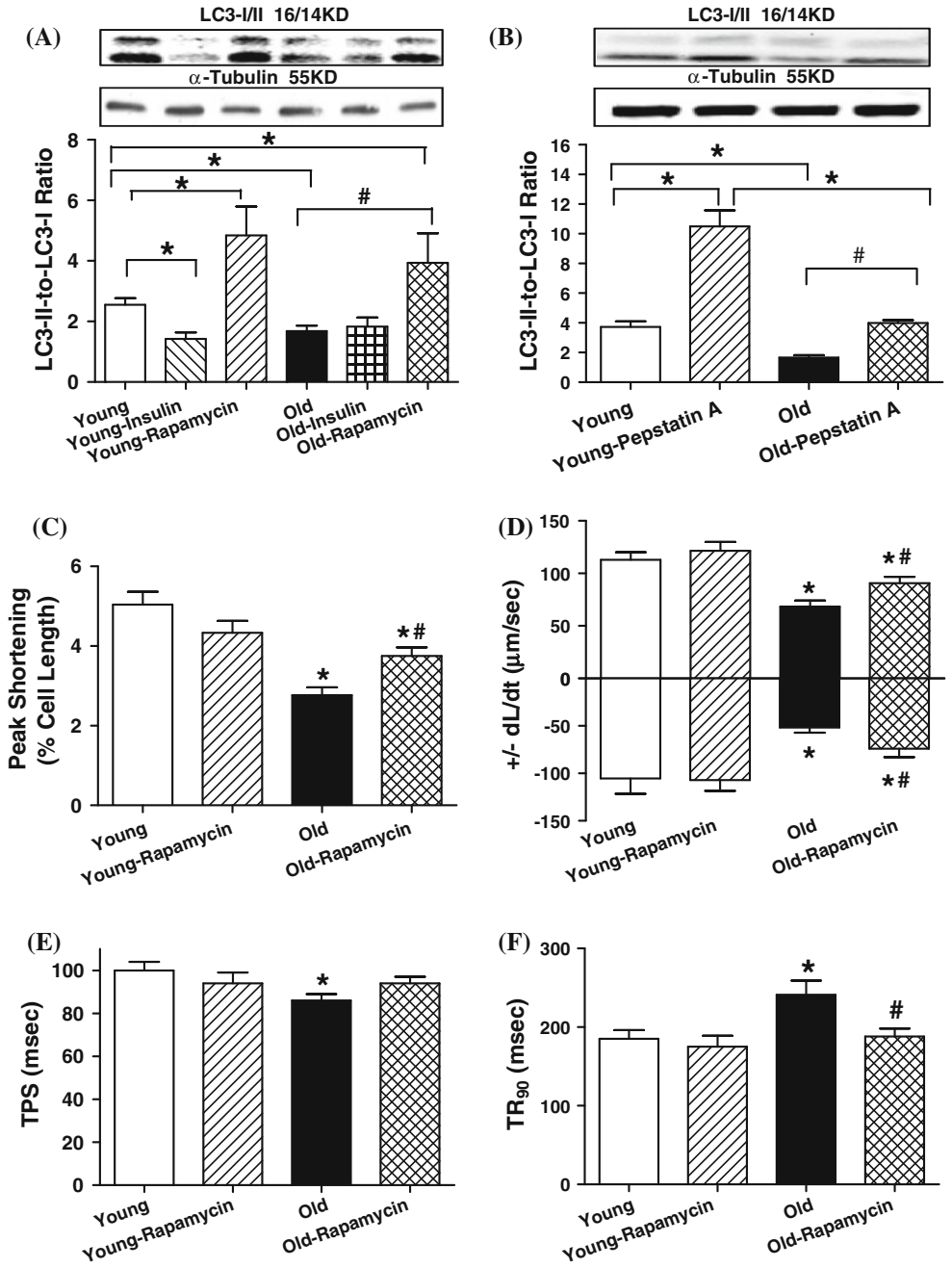

Fig. 9 Effect of Akt activation using insulin and lysosomal inhibition with pepstatin A on autophagy as well as the impact of autophagy induction on cardiomyocyte mechanical function in young (4 months) and old (24 months) WT mice. **a** LC3-II-to-LC3-I ratio in cardiomyocytes treated with or without the Akt activator insulin (100 nm, 15 min) or the autophagy inducer rapamycin (5 μM, 1 h) before immunoblotting was performed, **b** LC3-II-to-LC3-I ratio in cardiomyocytes from young and old mice treated with or without pepstatin a (10 μg/ml, 1 h) prior to immunoblotting, **c**–**f** cardiomyocyte contractile function in cardiomyocytes incubated for 4 h in the absence or presence of rapamycin (5 μM) prior to mechanical assessment. **c** peak shortening (normalized to resting cell length), **d** maximal velocity of shortening/relengthening (±dL/dt), **e** time-to-PS (TPS), and **f** time-to-90% relengthening (TR_{90}). Mean ± SEM, $n = 4$–5 isolations (*panel a–b*) or 98–119 cells from 4 mice (*panel c–f*), $^{*}p < 0.05$ versus respective young group, $^{\#}p < 0.05$ versus old group

[36, 62]. This is in line with the unchanged fractional shortening in our aged WT hearts. However, this apparent compensation in aging disappeared following chronic Akt activation, consistent with the detrimental effects of Akt and its downstream signaling molecules such as GSK3β in certain pathological conditions such as hypertrophic and ischemia–reperfusion injuries [10, 15, 19, 46, 49]. Ventricular hypertrophy and fibrosis are common manifestations of the aging heart and may lead to heart failure [59]. Our data revealed more prominent changes in heart mass,

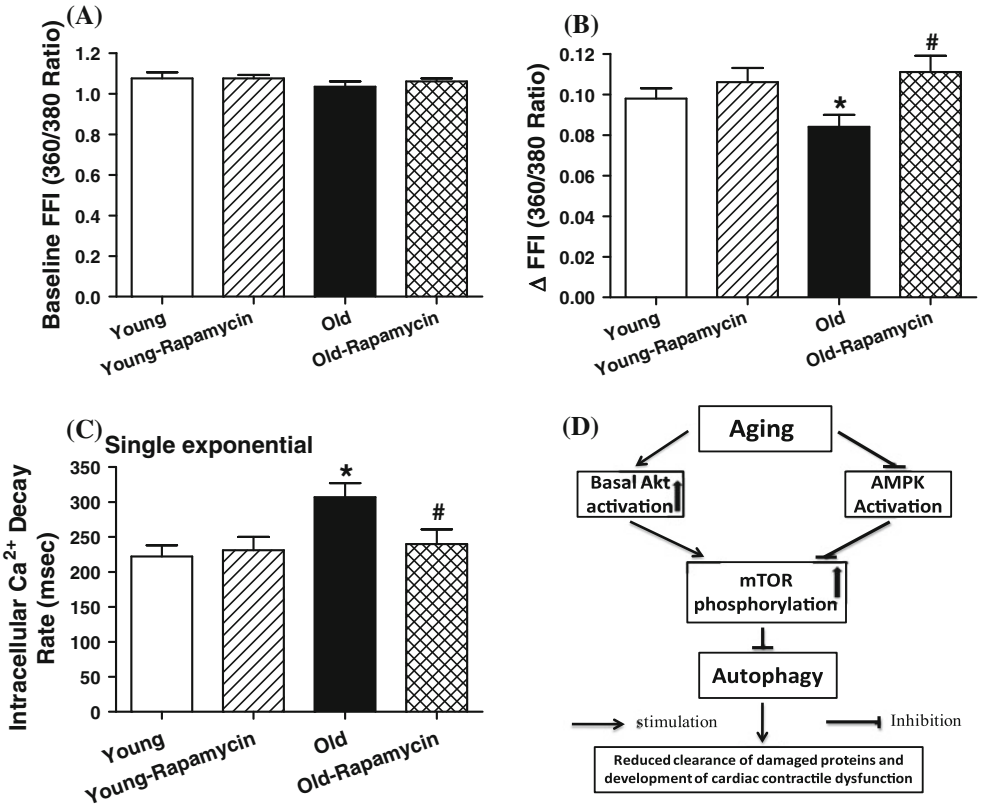

Fig. 10 Effect of autophagy induction on intracellular Ca^{2+} transient properties and proposed schematic diagrams of autophagy in cardiac aging. Isolated cardiomyocytes from young (4 months) and old (24 months) WT mice were incubated for 4 h in the absence or presence of rapamycin (5 μM) prior to assessment of intracellular Ca^{2+} handling. **a** Baseline FFI, **b** electrically stimulated rise in FFI (ΔFFI), **c** intracellular Ca^{2+} decay rate (single exponential), and **d** schematic illustration depicting the role of Akt, AMPK and mTOR in aging-induced changes in autophagy and cardiac contractile function. Mean ± SEM, $n = 72$ cells from 3 mice per group, $^{*}p < 0.05$ versus young group, $^{\#}p < 0.05$ versus old group

heart-to-body weight ratio, cardiomyocyte cross-sectional area, interstitial fibrosis and fractional shortening in aged Akt mice, favor a prominent role for Akt overactivation in aging as opposed to younger mice. EDD, which is preserved under aging and Akt activation, is significantly enhanced with concurrent aging and Akt overexpression. The enhanced EDD is likely responsible for reduced left ventricular fractional shortening in aged Akt mice. Our findings revealed increased ventricular wall thickness and ESD with aging, but not Akt overexpression, early on in life, suggesting a lesser role of short-term Akt overactivation in cardiac geometry and function. Although it is beyond the scope of our study to examine the precise mechanism responsible for cardiac hypertrophy in aged Akt mice, overexpression of the essential cardiac survival factor Akt may be responsible for exacerbated cardiac hypertrophy in these mice [10, 15]. It is worth mentioning that the young Akt transgenic mice exhibited comparable body and heart weight compared with their WT littermates, different from the earlier findings of enlarged body and heart mass (as well as larger cardiomyocyte surface area) using the same Akt transgenic mice [42]. This apparent discrepancy in mouse biometric data may be associated with the slightly younger age of mice in our study (3–4 months, mostly at 3 months of age) compared with those (15.4–15.8 weeks) previously reported [42].

In our study, aged murine cardiomyocytes displayed unchanged resting intracellular Ca^{2+} levels, decreased intracellular Ca^{2+} release in response to electrical stimulus (excitation) and delayed intracellular Ca^{2+} clearance, somewhat in line with our previous reports [38, 39, 61]. Although Akt overactivation did not affect intracellular Ca^{2+} homeostasis in young mice, it unveiled an overloaded resting and dampened release of intracellular Ca^{2+} with aging as well as accentuated aging-induced decrease in intracellular Ca^{2+} clearance. These findings suggest that Akt overactivation with time is capable of disrupting intracellular Ca^{2+} handling. Existence of intracellular Ca^{2+} mishandling in aging with or without chronic Akt activation is further supported by the reduced stress tolerance shown as a steeper negative staircase in peak shortening-frequency response. Dampened SERCA2a expression and phospholamban phosphorylation may account for, at least in part, intracellular Ca^{2+} mishandling, prolonged intracellular

Ca^{2+} clearance and cardiac relaxation in senescent Akt murine hearts although further study is warranted. Since Akt overexpression itself did not alter myocardial contractile and intracellular Ca^{2+} properties in young mouse hearts, activation of this kinase early on in life may not be innately harmful to cardiac function. It should be pointed out that the discrepant findings between unchanged fractional shortening and reduced cardiomyocyte contractile capacity in the aging WT group may be related to possible non-cardiomyocyte factors such as fibroblasts and connective tissues as well as the non-loading isotonic nature of our current in vitro experimental setting.

Akt overactivation worsens cardiac insulin signaling independent of the whole body metabolic status in aging

Several mechanisms may be proposed for chronic Akt activation-elicited exaggeration of aging-induced cardiac mechanical and intracellular Ca^{2+} dysregulation. First, our data revealed that chronic Akt overactivation exacerbated aging-induced decrease in cardiac glucose uptake, depicting an involvement of glucose metabolism and fatty acid uptake in Akt overexpression-elicited cardiac geometric and functional anomalies. Aging-induced decrease in the expression of Glut4 has been demonstrated [58]. Findings using the same murine model revealed that chronic Akt activation dampened insulin-stimulated glucose uptake in adulthood [43], reminiscent of our current findings. However, the more dramatic reduction in insulin-stimulated glucose uptake does not seem to be associated with any dramatic increases in blood glucose, plasma insulin and/or HOMA-IR indices in aged Akt mice, suggesting that cardiac anomalies may develop independent of the whole body metabolic status (levels of fasting glucose, insulin and HOMA-IR). In addition, our data revealed upregulated insulin receptor β in aging WT mice which may be a possible compensatory response of the dampened insulin sensitivity with aging. The enhanced PDK1 phosphorylation in Akt mice is somewhat surprising and may reflect a feedback regulation of chronic Akt activation as PDK1 is known to activate Akt [45]. Our data depicted low phosphorylation of the Akt negative regulator PTEN with aging, the effect of which was accentuated by Akt overexpression. This finding favors a role for PTEN in the regulation of Akt activation in aging and chronic Akt overactivation states.

Akt activation worsens aging-induced decrease in autophagy possibly through mTOR and AMPK signaling in the heart

Perhaps the most interesting finding from our present study is that chronic Akt activation accentuates aging-induced decline in autophagy. This is shown by reduced autophagy protein markers and upregulated levels of insoluble p62. Akt is an essential regulator involved in cardiac survival and autophagy [51]. Numerous studies have demonstrated that Akt activation and aging may independently decrease autophagic activity [4, 12, 14, 29, 51, 56, 64]. Our study revealed that the autophagy inducer rapamycin improved aging-induced cardiomyocyte contractile and intracellular Ca^{2+} dysregulation. This is consistent with a recent report that rapamycin prolongs lifespan in a murine model through activation of autophagy [26]. In addition, long-term caloric restriction, a known trigger for autophagy induction [14, 60], overtly improves diastolic function in senescent myocardium through amelioration of the age-associated intracellular Ca^{2+} mishandling [53]. In vitro insulin treatment, which activates Akt, significantly suppressed autophagy in young but not in aged cardiomyocytes. These data suggest that Akt activation with time may inhibit autophagy in aging and thus elicit cardiac geometric and functional anomalies associated with aging. The lack of inhibition in autophagy in aged murine cardiomyocytes by insulin may be due to an already low basal autophagy level in aging. Our data depicted a significant increase in mTOR phosphorylation in aged mice which was in line with the enhanced Akt activation in these mice. These findings are supportive of the loss of autophagy in aged WT and Akt mice as mTOR negatively regulates autophagy and life span [5, 25, 52]. Nonetheless, further scrutiny is needed to elucidate the precise role for mTOR in aging-induced change in cardiac geometric and functional changes. In addition, mTOR may coordinate survival and growth in response to various stimuli independent of autophagy regulation [5, 25]. For example, mTOR complex I may participate in the aging process through promoting mRNA translation and ribosome biogenesis [25]. Our data also revealed reduced phosphorylation of AMPK and its target ACC in aged mice, the effect of which may be exacerbated by Akt overactivation. This finding supports the inverse correlation between AMPK and Akt signaling [34]. AMPK has been shown to regulate intracellular fatty acid oxidation via inactivating ACC (phosphorylation of ACC) [35]. The aging-induced suppression of AMPK phosphorylation was shown previously [37]. AMPK may be negatively regulated by Akt phosphorylation while the duo often exert opposite pleiotropic and metabolic responses in the heart [40]. Aging-associated decreases in AMPK phosphorylation observed in our study may provide an alternate mechanism for the low level of autophagy in aging. AMPK is known to promote autophagy and an array of cardiac responses through inhibition of mTOR [40, 65]. Changes in pACC levels during aging not only provide evidence that Akt plays a role in aging-associated intracellular fat oxidation and insulin signaling, but also suggest

involvement of an AMPK-ACC-mTOR mediated pathway in Akt overactivation-exacerbated aging responses. Although the nature of the ACC pathway is beyond the scope of our current study, its important role in cardiac aging should not be underestimated. Last, but not least, our data failed to reveal any patterns of responsiveness to eNOS expression, not favoring a major role for eNOS in aging and/or Akt overactivation-induced cardiac responses. A scheme is shown to illustrate the possible mechanisms of action in Akt- and AMPK-induced regulation of autophagy with mTOR serving as a converging point en route to protein quality control in the heart and therefore regulation of cardiac contractile function (Fig. 10d).

Role of lysosomal pathways in Akt activation accentuated autophagic response in aging heart

Detection of processed LC3-II is an important approach to quantify autophagy [14, 21, 40]. However, measurement of the LC3-II-to-LC3-I ratio may not be the best parameter to estimate autophagic status. Our current data revealed a lower LC3-II-to-LC3-I ratio in aged cardiomyocytes in the absence (steady-state autophagosomes) or presence (cumulative autophagosomes) of the lysosomal inhibitor pepstatin A, suggesting a minor role for lysosomal degradation (i.e., the late-stage autophagic flux) in aging-induced decrease in autophagy. This is somewhat supported by the negative findings from the β-glucuronidase activity and cathepsin B experiments. Interestingly, our study revealed reduced LAMP1 expression in aged WT but not Akt transgenic mice. LAMP1 is a lysosomal membrane receptor protein to mediate the fusion of mature autophagosomes with cytosolic lysosomes forming autophagolysosomes prior to the hydrolysis of the sequestered component [17]. Levels of LAMP1 were found to be reduced in aging hearts [60], consistent with our present findings. Nonetheless, our data do not favor a role for LAMP1 in Akt overactivation-induced cardiac autophagic and mechanical responses. It is worth mentioning that increased insoluble p62 levels in aging with a more pronounced response in Akt transgenic also support a role for poor early stage autophagosome formation in aging- and Akt overactivation-induced autophagic responses. Levels of p62 are used to assess autophagic flux. The autophagy adaptor bridges ubiquitinated proteins to LC3 and becomes Triton-insoluble itself prior to incorporation into autophagosomes and degradation by lysosomes [31]. Therefore, our observation of accumulation of insoluble p62 depicts impaired autophagic pathway in aging and Akt overactivation. Finally, it is noteworthy that the aging markers lipofuscin were elevated in a comparable manner in both WT and Akt murine hearts, suggesting possible contribution of autophagy-independent mechanism(s) such as ubiquitin–proteasome system to the accumulation of the garbage protein aggregates in aging [32].

In summary, our findings suggest that Akt may play an essential role in the regulation of cardiac function in the elderly. Our data favor the notion that increased Akt phosphorylation with aging may be responsible for reduced autophagic activity in aging, indicating the therapeutic potentials for Akt and autophagy in the management of aging-associated complications. Although our study sheds some light on the interaction of Akt/AMPK/mTOR signaling, autophagy and aging-induced cardiac geometric, functional and intracellular Ca^{2+} defects, the pathogenesis of cardiac dysfunction under aging, particularly in association with autophagy, still deserves further investigation.

Acknowledgments The authors wish to acknowledge the technical assistance of Ms. Lisa Li from the University of Wyoming. This work was supported in part by NIH/NCRR P20 RR016474.

References

1. Alvers AL, Fishwick LK, Wood MS, Hu D, Chung HS, Dunn WA Jr, Aris JP (2009) Autophagy and amino acid homeostasis are required for chronological longevity in *Saccharomyces cerevisiae*. Aging Cell 8:353–369. doi:10.1111/j.1474-9726.2009.00469.x
2. Baudhuin P (1966) Lysosomes and cellular autophagy. Brux Med 46:1059–1070
3. Birnbaum Y, Long B, Qian J, Perez-Polo JR, Ye Y (2011) Pioglitazone limits myocardial infarct size, activates Akt, and upregulates cPLA2 and COX-2 in a PPAR-gamma-independent manner. Basic Res Cardiol 106:431–446. doi:10.1007/s00395-011-0162-3
4. Bjedov I, Toivonen JM, Kerr F, Slack C, Jacobson J, Foley A, Partridge L (2010) Mechanisms of life span extension by rapamycin in the fruit fly *Drosophila melanogaster*. Cell Metab 11:35–46. doi:10.1016/j.cmet.2009.11.010
5. Blagosklonny MV (2008) Aging: ROS or TOR. Cell Cycle 7:3344–3354. doi:10.4161/cc.7.21.6965
6. Boengler K, Buechert A, Heinen Y, Roeskes C, Hilfiker-Kleiner D, Heusch G, Schulz R (2008) Cardioprotection by ischemic postconditioning is lost in aged and STAT3-deficient mice. Circ Res 102:131–135. doi:10.1161/CIRCRESAHA.107.164699
7. Boengler K, Konietzka I, Buechert A, Heinen Y, Garcia-Dorado D, Heusch G, Schulz R (2007) Loss of ischemic preconditioning's cardioprotection in aged mouse hearts is associated with reduced gap junctional and mitochondrial levels of connexin 43. Am J Physiol Heart Circ Physiol 292:H1764–H1769. doi:10.1152/ajpheart.01071.2006
8. Boengler K, Schulz R, Heusch G (2009) Loss of cardioprotection with ageing. Cardiovasc Res 83:247–261. doi:10.1093/cvr/cvp033
9. Breivik L, Helgeland E, Aarnes EK, Mrdalj J, Jonassen AK (2011) Remote postconditioning by humoral factors in effluent from ischemic preconditioned rat hearts is mediated via PI3K/Akt-dependent cell-survival signaling at reperfusion. Basic Res Cardiol 106:135–145. doi:10.1007/s00395-010-0133-0
10. Carneiro-Ramos MS, Diniz GP, Nadu AP, Almeida J, Vieira RL, Santos RA, Barreto-Chaves ML (2010) Blockage of angiotensin

II type 2 receptor prevents thyroxine-mediated cardiac hypertrophy by blocking Akt activation. Basic Res Cardiol 105:325–335. doi:10.1007/s00395-010-0089-0
11. Ceylan-Isik AF, Zhao P, Zhang B, Xiao X, Su G, Ren J (2010) Cardiac overexpression of metallothionein rescues cardiac contractile dysfunction and endoplasmic reticulum stress but not autophagy in sepsis. J Mol Cell Cardiol 48:367–378. doi:10.1016/j.yjmcc.2009.11.003
12. Cuervo AM, Bergamini E, Brunk UT, Droge W, Ffrench M, Terman A (2005) Autophagy and aging: the importance of maintaining "clean" cells. Autophagy 1:131–140. doi:10.4161/auto.1.3.2017
13. Davidoff AJ, Mason MM, Davidson MB, Carmody MW, Hintz KK, Wold LE, Podolin DA, Ren J (2004) Sucrose-induced cardiomyocyte dysfunction is both preventable and reversible with clinically relevant treatments. Am J Physiol Endocrinol Metab 286:E718–E724. doi:10.1152/ajpendo.00358.2003
14. De Meyer GR, De Keulenaer GW, Martinet W (2010) Role of autophagy in heart failure associated with aging. Heart Fail Rev 15:423–430. doi:10.1007/s10741-010-9166-6
15. Diniz GP, Carneiro-Ramos MS, Barreto-Chaves ML (2009) Angiotensin type 1 receptor mediates thyroid hormone-induced cardiomyocyte hypertrophy through the Akt/GSK-3beta/mTOR signaling pathway. Basic Res Cardiol 104:653–667. doi:10.1007/s00395-009-0043-1
16. Doser TA, Turdi S, Thomas DP, Epstein PN, Li SY, Ren J (2009) Transgenic overexpression of aldehyde dehydrogenase-2 rescues chronic alcohol intake-induced myocardial hypertrophy and contractile dysfunction. Circulation 119:1941–1949. doi:10.1161/CIRCULATIONAHA.108.823799
17. Eskelinen EL (2006) Roles of LAMP-1 and LAMP-2 in lysosome biogenesis and autophagy. Mol Aspects Med 27:495–502. doi:10.1016/j.mam.2006.08.005
18. Fujita K, Maeda D, Xiao Q, Srinivasula SM (2011) Nrf2-mediated induction of p62 controls Toll-like receptor-4-driven aggresome-like induced structure formation and autophagic degradation. Proc Natl Acad Sci USA 108:1427–1432. doi:10.1073/pnas.1014156108
19. Ghaboura N, Tamareille S, Ducluzeau PH, Grimaud L, Loufrani L, Croue A, Tourmen Y, Henrion D, Furber A, Prunier F (2011) Diabetes mellitus abrogates erythropoietin-induced cardioprotection against ischemic-reperfusion injury by alteration of the RISK/GSK-3beta signaling. Basic Res Cardiol 106:147–162. doi:10.1007/s00395-010-0130-3
20. Goswami SK, Das DK (2006) Autophagy in the myocardium: dying for survival? Exp Clin Cardiol 11:183–188
21. Gottlieb RA, Finley KD, Mentzer RM Jr (2009) Cardioprotection requires taking out the trash. Basic Res Cardiol 104:169–180. doi:10.1007/s00395-009-0011-9
22. Ha SD, Ham B, Mogridge J, Saftig P, Lin S, Kim SO (2010) Cathepsin B-mediated autophagy flux facilitates the anthrax toxin receptor 2-mediated delivery of anthrax lethal factor into the cytoplasm. J Biol Chem 285:2120–2129. doi:10.1074/jbc.M109.065813
23. Hahn-Windgassen A, Nogueira V, Chen CC, Skeen JE, Sonenberg N, Hay N (2005) Akt activates the mammalian target of rapamycin by regulating cellular ATP level and AMPK activity. J Biol Chem 280:32081–32089. doi:10.1074/jbc.M502876200
24. Hamacher-Brady A, Brady NR, Gottlieb RA (2006) Enhancing macroautophagy protects against ischemia/reperfusion injury in cardiac myocytes. J Biol Chem 281:29776–29787. doi:10.1074/jbc.M603783200
25. Hands SL, Proud CG, Wyttenbach A (2009) mTOR's role in ageing: protein synthesis or autophagy? Aging (Albany NY) 1:586–597
26. Harrison DE, Strong R, Sharp ZD, Nelson JF, Astle CM, Flurkey K, Nadon NL, Wilkinson JE, Frenkel K, Carter CS, Pahor M, Javors MA, Fernandez E, Miller RA (2009) Rapamycin fed late in life extends lifespan in genetically heterogeneous mice. Nature 460:392–395. doi:10.1038/nature08221
27. Hars ES, Qi H, Ryazanov AG, Jin S, Cai L, Hu C, Liu LF (2007) Autophagy regulates ageing in *C. elegans*. Autophagy 3:93–95
28. Hay N, Sonenberg N (2004) Upstream and downstream of mTOR. Genes Dev 18:1926–1945. doi:10.1101/gad.1212704
29. Iida RH, Kanko S, Suga T, Morito M, Yamane A (2011) Autophagic-lysosomal pathway functions in the masseter and tongue muscles in the klotho mouse, a mouse model for aging. Mol Cell Biochem 348:89–98. doi:10.1007/s11010-010-0642-z
30. Inuzuka Y, Okuda J, Kawashima T, Kato T, Niizuma S, Tamaki Y, Iwanaga Y, Yoshida Y, Kosugi R, Watanabe-Maeda K, Machida Y, Tsuji S, Aburatani H, Izumi T, Kita T, Shioi T (2009) Suppression of phosphoinositide 3-kinase prevents cardiac aging in mice. Circulation 120:1695–1703. doi:10.1161/CIRCULATIONAHA.109.871137
31. Johansen T, Lamark T (2011) Selective autophagy mediated by autophagic adapter proteins. Autophagy 7:279–296. doi:10.4161/auto.7.3.14487
32. Kanaan NM, Kordower JH, Collier TJ (2007) Age-related accumulation of Marinesco bodies and lipofuscin in rhesus monkey midbrain dopamine neurons: relevance to selective neuronal vulnerability. J Comp Neurol 502:683–700. doi:10.1002/cne.21333
33. Koldovsky O (1971) Developmental changes of beta-galactosidase and beta-glucuronidase in the rat liver and kidney. Arch Biochem Biophys 142:378–381
34. Kovacic S, Soltys CL, Barr AJ, Shiojima I, Walsh K, Dyck JR (2003) Akt activity negatively regulates phosphorylation of AMP-activated protein kinase in the heart. J Biol Chem 278:39422–39427. doi:10.1074/jbc.M305371200
35. Kudo N, Barr AJ, Barr RL, Desai S, Lopaschuk GD (1995) High rates of fatty acid oxidation during reperfusion of ischemic hearts are associated with a decrease in malonyl-CoA levels due to an increase in 5′-AMP-activated protein kinase inhibition of acetyl-CoA carboxylase. J Biol Chem 270:17513–17520
36. Lakatta EG (1999) Cardiovascular aging research: the next horizons. J Am Geriatr Soc 47:613–625
37. Li Q, Ceylan-Isik AF, Li J, Ren J (2008) Deficiency of insulin-like growth factor 1 reduces sensitivity to aging-associated cardiomyocyte dysfunction. Rejuvenation Res 11:725–733. doi:10.1089/rej.2008.0717
38. Li Q, Ren J (2007) Influence of cardiac-specific overexpression of insulin-like growth factor 1 on lifespan and aging-associated changes in cardiac intracellular Ca^{2+} homeostasis, protein damage and apoptotic protein expression. Aging Cell 6:799–806. doi:10.1111/j.1474-9726.2007.00343.x
39. Li Q, Wu S, Li SY, Lopez FL, Du M, Kajstura J, Anversa P, Ren J (2007) Cardiac-specific overexpression of insulin-like growth factor 1 attenuates aging-associated cardiac diastolic contractile dysfunction and protein damage. Am J Physiol Heart Circ Physiol 292:H1398–H1403. doi:10.1152/ajpheart.01036.2006
40. Ma H, Guo R, Yu L, Zhang Y, Ren J (2011) Aldehyde dehydrogenase 2 (ALDH2) rescues myocardial ischaemia/reperfusion injury: role of autophagy paradox and toxic aldehyde. Eur Heart J 32:1025–1038. doi:10.1093/eurheartj/ehq253
41. Matarrese P, Nencioni L, Checconi P, Ciarlo L, Gambardella L, Ascione B, Sgarbanti R, Garaci E, Malorni W, Palamara AT (2011) Pepstatin a alters host cell autophagic machinery and leads to a decrease in influenza a virus production. J Cell Physiol. doi:10.1002/jcp.22696

42. Matsui T, Li L, Wu JC, Cook SA, Nagoshi T, Picard MH, Liao R, Rosenzweig A (2002) Phenotypic spectrum caused by transgenic overexpression of activated Akt in the heart. J Biol Chem 277:22896–22901. doi:10.1074/jbc.M200347200
43. Matsui T, Nagoshi T, Hong EG, Luptak I, Hartil K, Li L, Gorovits N, Charron MJ, Kim JK, Tian R, Rosenzweig A (2006) Effects of chronic Akt activation on glucose uptake in the heart. Am J Physiol Endocrinol Metab 290:E789–E797. doi:10.1152/ajpendo.00564.2004
44. Matthews DR, Hosker JP, Rudenski AS, Naylor BA, Treacher DF, Turner RC (1985) Homeostasis model assessment: insulin resistance and beta-cell function from fasting plasma glucose and insulin concentrations in man. Diabetologia 28:412–419
45. Miyamoto S, Murphy AN, Brown JH (2009) Akt mediated mitochondrial protection in the heart: metabolic and survival pathways to the rescue. J Bioenerg Biomembr 41:169–180. doi:10.1007/s10863-009-9205-y
46. Nagoshi T, Matsui T, Aoyama T, Leri A, Anversa P, Li L, Ogawa W, del Monte F, Gwathmey JK, Grazette L, Hemmings BA, Kass DA, Champion HC, Rosenzweig A (2005) PI3K rescues the detrimental effects of chronic Akt activation in the heart during ischemia/reperfusion injury. J Clin Invest 115:2128–2138. doi:10.1172/JCI23073
47. Nakai A, Yamaguchi O, Takeda T, Higuchi Y, Hikoso S, Taniike M, Omiya S, Mizote I, Matsumura Y, Asahi M, Nishida K, Hori M, Mizushima N, Otsu K (2007) The role of autophagy in cardiomyocytes in the basal state and in response to hemodynamic stress. Nat Med 13:619–624. doi:10.1038/nm1574
48. Oudit GY, Penninger JM (2009) Cardiac regulation by phosphoinositide 3-kinases and PTEN. Cardiovasc Res 82:250–260. doi:10.1093/cvr/cvp014
49. Penna C, Tullio F, Perrelli MG, Moro F, Abbadessa G, Piccione F, Carriero V, Racca S, Pagliaro P (2011) Ischemia/reperfusion injury is increased and cardioprotection by a postconditioning protocol is lost as cardiac hypertrophy develops in nandrolone treated rats. Basic Res Cardiol 106:409–420. doi:10.1007/s00395-010-0143-y
50. Qian J, Ren X, Wang X, Zhang P, Jones WK, Molkentin JD, Fan GC, Kranias EG (2009) Blockade of Hsp20 phosphorylation exacerbates cardiac ischemia/reperfusion injury by suppressed autophagy and increased cell death. Circ Res 105:1223–1231. doi:10.1161/CIRCRESAHA.109.200378
51. Ronnebaum SM, Patterson C (2010) The FoxO family in cardiac function and dysfunction. Annu Rev Physiol 72:81–94. doi:10.1146/annurev-physiol-021909-135931
52. Sarkar S, Ravikumar B, Floto RA, Rubinsztein DC (2009) Rapamycin and mTOR-independent autophagy inducers ameliorate toxicity of polyglutamine-expanded huntingtin and related proteinopathies. Cell Death Differ 16:46–56. doi:10.1038/cdd.2008.110
53. Shinmura K, Tamaki K, Sano M, Murata M, Yamakawa H, Ishida H, Fukuda K (2011) Impact of long-term caloric restriction on cardiac senescence: caloric restriction ameliorates cardiac diastolic dysfunction associated with aging. J Mol Cell Cardiol 50:117–127. doi:10.1016/j.yjmcc.2010.10.018
54. Simonsen A, Cumming RC, Brech A, Isakson P, Schubert DR, Finley KD (2008) Promoting basal levels of autophagy in the nervous system enhances longevity and oxidant resistance in adult *Drosophila*. Autophagy 4:176–184
55. Sussman MA, Anversa P (2004) Myocardial aging and senescence: where have the stem cells gone? Annu Rev Physiol 66:29–48. doi:10.1146/annurev.physiol.66.032102.140723
56. Taneike M, Yamaguchi O, Nakai A, Hikoso S, Takeda T, Mizote I, Oka T, Tamai T, Oyabu J, Murakawa T, Nishida K, Shimizu T, Hori M, Komuro I, Shirasawa T, Mizushima N, Otsu K (2010) Inhibition of autophagy in the heart induces age-related cardiomyopathy. Autophagy 6:600–606. doi:10.4161/auto.6.5.11947
57. Toth ML, Sigmond T, Borsos E, Barna J, Erdelyi P, Takacs-Vellai K, Orosz L, Kovacs AL, Csikos G, Sass M, Vellai T (2008) Longevity pathways converge on autophagy genes to regulate life span in *Caenorhabditis elegans*. Autophagy 4:330–338
58. Vettor R, Fabris R, Serra R, Lombardi AM, Tonello C, Granzotto M, Marzolo MO, Carruba MO, Ricquier D, Federspil G, Nisoli E (2002) Changes in FAT/CD36, UCP2, UCP3 and GLUT4 gene expression during lipid infusion in rat skeletal and heart muscle. Int J Obes Relat Metab Disord 26:838–847. doi:10.1038/sj.ijo.0802005
59. Wei JY (1992) Age and the cardiovascular system. N Engl J Med 327:1735–1739. doi:10.1056/NEJM199212103272408
60. Wohlgemuth SE, Julian D, Akin DE, Fried J, Toscano K, Leeuwenburgh C, Dunn WA Jr (2007) Autophagy in the heart and liver during normal aging and calorie restriction. Rejuvenation Res 10:281–292. doi:10.1089/rej.2006.0535
61. Yang X, Doser TA, Fang CX, Nunn JM, Janardhanan R, Zhu M, Sreejayan N, Quinn MT, Ren J (2006) Metallothionein prolongs survival and antagonizes senescence-associated cardiomyocyte diastolic dysfunction: role of oxidative stress. FASEB J 20:1024–1026. doi:10.1096/fj.05-5288fje
62. Yang X, Sreejayan N, Ren J (2005) Views from within and beyond: narratives of cardiac contractile dysfunction under senescence. Endocrine 26:127–137. doi:10.1385/ENDO:26:2:127
63. Yitzhaki S, Huang C, Liu W, Lee Y, Gustafsson AB, Mentzer RM Jr, Gottlieb RA (2009) Autophagy is required for preconditioning by the adenosine A1 receptor-selective agonist CCPA. Basic Res Cardiol 104:157–167. doi:10.1007/s00395-009-0006-6
64. Zhang C, Cuervo AM (2008) Restoration of chaperone-mediated autophagy in aging liver improves cellular maintenance and hepatic function. Nat Med 14:959–965. doi:10.1038/nm.1851
65. Zhang Y, Ren J (2010) Autophagy in ALDH2-elicited cardioprotection against ischemic heart disease: slayer or savior? Autophagy 6:1212–1213. doi:10.4161/auto.6.8.13652
66. Zhang Y, Zeng Y, Wang M, Tian C, Ma X, Chen H, Fang Q, Jia L, Du J, Li H (2011) Cardiac-specific overexpression of E3 ligase Nrdp1 increases ischemia and reperfusion-induced cardiac injury. Basic Res Cardiol 106:371–383. doi:10.1007/s00395-011-0157-0